

Supporting information for

Rapid Selective Circumneutral Degradation of Phenolic Pollutants Using Peroxymonosulfate-Iodide Metal-Free Oxidation: Role of Iodine Atoms

Yong Feng^a, Po-Heng Lee^b, Deli Wu^c, Kaimin Shih^{a,*}

^a Department of Civil Engineering, The University of Hong Kong, Pokfulam, Hong Kong

^b Department of Civil and Environmental Engineering, The Hong Kong Polytechnic University, Hung Hom, Hong Kong

^c State Key Laboratory of Pollution Control and Resources Reuse, School of Environmental Science & Engineering, Tongji University, Shanghai 200092, People's Republic of China

Environmental Science & Technology

Revised in January, 2017

Contact information:

Yong Feng (fengy@hku.hk)

Po-Heng Lee (phlee@polyu.edu.hk)

Deli Wu (wudeli@tongji.edu.cn)

Kaimin Shih (kshih@hku.hk)

* To whom correspondence should be addressed:

Dr. Kaimin Shih

Phone: +852-2859-1973

Fax: +852-2559-5337

E-mail: kshih@hku.hk

Totally 19 pages including 4 Text, 5 Tables, and 12 Figures.

List of supporting information

Text S1. Effect of background ionic strength.

Text S2. Analysis of the selected pollutants.

Text S3. Identification and quantification of degradation intermediates.

Text S4. Quantification of oxygen-containing radicals with the methanol probe method.

Table S1. Halide ions in various water sources.

Table S2. Physicochemical properties of the selected pollutants.

Table S3. Rate constants of sulfite oxidation by oxidative species.

Table S4. UPLC-PDA conditions for pollutant analysis.

Table S5. UPLC-MS/MS conditions for iodophenols.

Figure S1. Effect of phosphate buffer on the degradation of phenol by PMS- I^- oxidation. Conditions: [phenol] = 10 μ M, [PMS] = 65 μ M, [NaH₂PO₄] = 1 mM, [Na₂SO₄] = 10 mM, and [I^-] = 50 μ M.

Figure S2. Degradation of pollutants by PMS alone. Conditions: [PMS] = 65 μ M, [phenol] = [2,4-dichlorophenol] = [bisphenol A] = [chloramphenicol] = [atrazine] = [nitrobenzene] = [methylene blue] = [hydroquinone] = 10 μ M, [Na₂SO₄] = 10 mM, and initial solution pH = 6.0.

Figure S3. Concentrations of phenol and atrazine versus reaction time in PMS- I^- oxidation. Conditions: [PMS] = 65 μ M, [I^-] = 50 μ M, [phenol] = [atrazine] = 25 μ M, [Na₂SO₄] = 10 mM, and initial solution pH = 6.0.

Figure S4. Plot of $-\ln(C/C_0)$ versus reaction time (min) during phenol (a), bisphenol A (b), and 2,4-dichlorophenol (c) degradation in PMS- I^- oxidation. Conditions: [PMS] = 65 μ M, [I^-] = 50 μ M, [phenol] = [bisphenol A] = [2,4-dichlorophenol] = 10 μ M, [Na₂SO₄] = 10 mM, and initial solution pH = 6.0. Duplicate experiments were carried out and the slope represents the pseudo-first-order constant.

Figure S5. Effect of methanol on the degradation of phenol by PMS-Co²⁺ oxidation. Conditions: [PMS] = 65 μ M, [Co(NO₃)₂] = 65 μ M, [phenol] = 25 μ M, and initial solution pH = 6.0.

Figure S6. Effect of sodium azide on the degradation of phenol by PMS- I^- oxidation. Conditions: [PMS] = 65 μ M, [I^-] = 50 μ M, [phenol] = 10 μ M, [sodium azide] = 10 μ M, [Na₂SO₄] = 10 mM, and initial solution pH = 6.0.

Figure S7. Effect of NH_4^+ on the degradation of phenol by PMS- I^- oxidation. Conditions: $[\text{PMS}] = 65 \mu\text{M}$, $[\text{I}^-] = 50 \mu\text{M}$, $[\text{phenol}] = 25 \mu\text{M}$, $[\text{Na}_2\text{SO}_4] = 10 \text{ mM}$, and initial solution pH 6.0.

Figure S8. Degradation of phenols by PMS- I^- oxidation when a significant excess of I^- was present. Conditions: $[\text{PMS}] = 65 \mu\text{M}$, $[\text{I}^-] = 10 \text{ mM}$, $[\text{phenol}] = [\text{2,4-diclorophenol}] = 10 \mu\text{M}$, $[\text{Na}_2\text{SO}_4] = 10 \text{ mM}$, and initial solution pH = 6.0.

Figure S9. (a) Effect of resorcinol on the color of PMS- I^- oxidation and (b) the reactors in (a) after adding starch; the yellow color indicates the formation of I_3^- and the obvious color variation after adding starch indicates the presence of I_3^- . Conditions: $[\text{PMS}] = 100 \mu\text{M}$, $[\text{I}^-] = 500 \mu\text{M}$, $[\text{starch}] = 1 \text{ g L}^{-1}$, reaction time = 10 min, $[\text{Na}_2\text{SO}_4] = 10 \text{ mM}$, and initial solution pH = 6.0.

Figure S10. Profile of major iodinated intermediates produced during phenol degradation by PMS- I^- oxidation and their percent yield. Conditions: $[\text{PMS}] = 65 \mu\text{M}$, $[\text{I}^-] = 50 \mu\text{M}$, $[\text{phenol}] = 10 \mu\text{M}$, $[\text{Na}_2\text{SO}_4] = 10 \text{ mM}$, and initial solution pH = 6.0.

Figure S11. Phenol degradation in PMS solution in the presence of both Br^- and I^- . Conditions: $[\text{PMS}] = 65 \mu\text{M}$, $[\text{Br}^-] = 3.65 \mu\text{M}$, $[\text{I}^-] = 0.5 \mu\text{M}$, $[\text{phenol}] = 25 \mu\text{M}$, $[\text{Na}_2\text{SO}_4] = 10 \text{ mM}$, and initial solution pH 6.0; the doses of Br^- and I^- were based on their maximum weight ratios in the supplied sodium chloride (0.001% I^- and 0.01% Br^-) under the condition of 50 mM Cl^- .

Figure S12. Effect of HCO_3^- on atrazine degradation in PMS- I^- oxidation. Conditions: $[\text{PMS}] = 65 \mu\text{M}$, $[\text{I}^-] = 50 \mu\text{M}$, $[\text{atrazine}] = 10 \mu\text{M}$, $[\text{Na}_2\text{SO}_4] = 10 \text{ mM}$, and reaction time = 10 min. The solution pH value was adjusted to 6.0 after adding HCO_3^- .

Text S1. Effect of background ionic strength.

On the basis of the Debye–Hückel theory,¹ the interaction between mononegative PMS (HSO_5^-) and halide ions was expected to be influenced by ionic strength. In this study, a moderate background ionic strength was used (10 mM Na_2SO_4) throughout the degradation experiments. This value was high enough to isolate the variation of ionic strength that probably occurred during the solution pH adjustment. Usually NaClO_4 was used to provide ionic strength. However, due to the concern of KClO_4 (K^+ from Oxone) precipitation, Na_2SO_4 was used instead.

Text S2. Analysis of the selected pollutants.

Pollutants including bisphenol A, nitrobenzene, atrazine, chloramphenicol, phenol, hydroquinone, and 2,4-dichlorophenol were analyzed with an UPLC-PDA system. A mixture containing ultrapure water and Optima LC-MS grade methanol was used as the mobile phase. The ratio of methanol, flow rate, retention time, and PDA detector wavelength for each compound were listed in Table S4. The column temperature was set at 50 °C and an injection volume of 10 μL was used. To determine the bisphenol A concentration in the presence of high levels of phenol (1 to 5 mM), a low flow rate of 0.2 mL min^{-1} was used to separate the two compounds. Other conditions were the same as that used for the bisphenol A analysis without phenol. To eliminate any matrix effect during the analysis, all calibration standard solutions were prepared in the presence of 10 mM Na_2SO_4 .

Text S3. Identification and quantification of degradation intermediates.

The identification of the degradation intermediates of phenol was realized by liquid-liquid extraction followed by GC-MS analysis. In a typical procedure, the degradation was first quenched by addition of excess sodium sulfite and the products were then separated by liquid-liquid extraction using dichloromethane as an extraction agent (2 mL dichloromethane into 40 mL reacting solutions). After agitation on a vortex mixer for 2 min, 1 μ L of the resulting organic solvent was used for GC-MS analysis. The GC-MS analysis was performed on an Agilent GC-MS (6890-5973) system equipped with a DB-5ms column (0.25 mm \times 30 m \times 0.25 μ m) and an auto sampler. The column temperature was initially held at 40 $^{\circ}$ C for 2 min, increased at 5 $^{\circ}$ C min $^{-1}$ to 150 $^{\circ}$ C and held for 1 min, and finally increased at 10 $^{\circ}$ C min $^{-1}$ to 260 $^{\circ}$ C and held for 2 min. The injector was operated in a split mode at a split ratio of 5:1 and the injector temperature was set at 280 $^{\circ}$ C. The electron ionization was carried out at an electron energy of 70 eV. A mass range from m/z 40 to 500 was recorded by operating the MS in the full-scan mode. The detector temperature was kept at 280 $^{\circ}$ C. On the basis of the total ion chromatogram, only 2-iodophenol, 3-iodophenol, and 2,4,6-triiodophenol were detected as the iodinated degradation intermediates of phenol.

To quantify the 2-iodophenol, 3-iodophenol, and 2,4,6-triiodophenol generated during the degradation of phenol by PMS-I $^{-}$ oxidation, the resulting organic extracts were monitored with UPLC-MS/MS. First, analytical protocols of these compounds were established by operating the MS/MS in multiple reaction monitoring (MRM) modes with electrospray ionization (ESI) as the ion source in the negative ion mode. Details about the MS/MS conditions are listed in Table S5. The quantification of these compounds was carried out by performing external calibration. Standard iodophenol stock solutions were prepared by dissolving iodophenols into acetone

($\geq 99.5\%$, BDH Chemicals). To mitigate matrix effects, the standard iodophenol stock solutions were diluted with dichloromethane. The detection limits were determined to be 0.045, 0.023, and $0.002 \mu\text{M}$ for 2-iodophenol, 3-iodophenol, and 2,4,6-triiodophenol, respectively. A mixture containing 2 mM ammonium acetate in methanol solution (5%, v/v) and 2 mM ammonium acetate in Optima LC-MS grade methanol at a volume ratio of 40:60 was used as the mobile phase and the separation was carried out at a flow rate of 0.4 mL min^{-1} and a column temperature of 50°C . Other chromatographic conditions were the same as that used for the analysis of phenols. Other MS parameters included a source temperature of 120°C , a desolvation temperature of 350°C , a desolvation gas flow of 600 L h^{-1} , a cone gas flow of 50 L h^{-1} , and capillary voltage of 0.50 kV. Argon (99.999%) was used as the collision gas, and its pressure in the collision cell was kept at $3.0 \times 10^{-3} \text{ mbar}$; nitrogen ($\geq 99.995\%$) was used as the cone and desolvation gas.

Text S4. Quantification of oxygen-containing radicals with the methanol probe method.

The quantification of both $\cdot\text{OH}$ and $\text{SO}_4^{\cdot-}$ was conducted with the methanol probe method.² Under the attack of these radicals, methanol was oxidized to formaldehyde, which was analyzed using a LC-PDA system after derivatization with 2,4-dinitrophenylhydrazine (DNPH) to form hydrazine (DNPH-HCHO). In a typical procedure, 40 mL of 1 M methanol solution at pH 6.0 was transferred to a 50-mL polypropylene centrifuge tube at room temperature ($23 \pm 2^\circ\text{C}$). Specified amounts of PMS and KI stock solutions were then added to the tube to initiate the oxidation. After reaction for 10 min, 0.5 mL of the solution was withdrawn and mixed with 200 μL DNPH (6 mM in acetonitrile) in 5 mL phosphate buffer (5 mM). After reaction for 30 min, 1 mL of the solution was used for formaldehyde analysis. The LC-PDA parameters are as follows: A mobile phase containing Optima LC-MS grade methanol and water at a volume ratio of 60:40, a flow rate of 0.4

mL min⁻¹, and a PDA detector wavelength at 355 nm. The retention time for DNPH and DNPH-HCHO were 0.91 and 2.15 min, respectively.

Table S1 Halide ions in various water sources

Water matrices	[I ⁻] (μ M)	[Cl ⁻] [mM]	[Br ⁻] [mM]
surface water	(0.004 to 1.67) ^{a 3}	(0.09 to 0.14) ⁴	$((0.17 \text{ to } 2.5) \times 10^{-3})$ ⁵
groundwater	(1.2 to 9.6) ^{a 6, 7}	(0.28 to 0.42) ⁸	0.069 ⁹
reverse osmosis concentrate	3.9 ¹⁰	39.0 ¹⁰	0.02 ¹⁰
landfill leachate	17.6 ¹¹	36.4 ¹²	(8.9×10^{-3}) ¹²
seawater	(0.4 to 0.5) ^{a 7}	545 ¹³	0.81 ⁵
oil and gas wastewater	(140 to 280) ¹⁴	(169 to 338) ¹⁵	(0.39 to 12.5) ¹⁵

^a total iodine concentration.

Table S2 Physicochemical properties of the selected pollutants

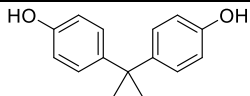
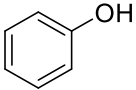
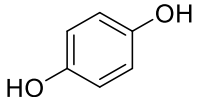
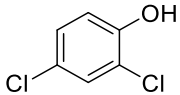
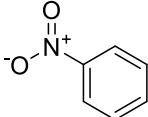
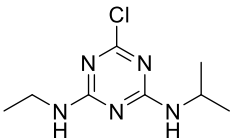
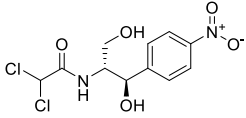
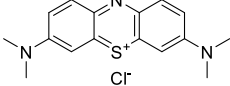
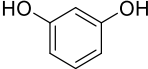
Compounds	Formula	p <i>K</i> _a	Molar mass (g mol ⁻¹)	Structure
bisphenol A	C ₁₅ H ₁₆ O ₂	9.73 ¹⁶	228.3	
phenol	C ₆ H ₆ O	9.9 ¹⁷	94.1	
hydroquinone	C ₆ H ₆ O ₂	9.85 ¹⁸	110.1	
2,4-dichlorophenol	C ₆ H ₄ Cl ₂ O	7.8 ¹⁷	163.0	
nitrobenzene	C ₆ H ₅ NO ₂	-12.44 ¹⁹	123.1	
atrazine	C ₈ H ₁₄ ClN ₅	1.7 ²⁰	215.7	
chloramphenicol	C ₁₁ H ₁₂ Cl ₂ N ₂ O ₅	5.5 ²¹	323.1	
methylene blue	C ₁₆ H ₁₈ ClN ₃ S	~	319.9	
resorcinol	C ₆ H ₆ O ₂	9.36 ²²	110.1	

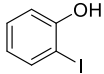
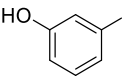
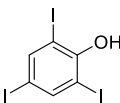
Table S3 Rate constants of sulfite oxidation by oxidative species

Reactions	Second-order constants (M ⁻¹ s ⁻¹)
SO ₃ ²⁻ + Cl ₂ ⁻ → products	(3.3 × 10 ⁷) ²³
SO ₃ ²⁻ + Br ₂ ⁻ → products	(6.9 × 10 ⁷ to 2.6 × 10 ⁸) ²⁴
SO ₃ ²⁻ + CO ₃ ⁻ → products	(3.3 × 10 ⁷) ²⁴
SO ₃ ²⁻ + ·OH → products	((5.5 to 9.5) × 10 ⁹) ²⁴
SO ₃ ²⁻ + SO ₄ ⁻ → products	(7.0 × 10 ⁸ to 1.1 × 10 ⁹) ²⁵
SO ₃ ²⁻ + SO ₅ ⁻ → products	(1.3 × 10 ⁷) ²⁶

Table S4 UPLC-PDA conditions for pollutant analysis

Compounds	Methanol/ water (v/v)	Wavelength (nm)	Detection limit (μM)	Calibration range (μM)	Retention time (min)
bisphenol A	60/40	226	0.28	2–30	0.67
nitrobenzene	60/40	264	0.32	1–12	0.68
atrazine	60/40	222	0.18	1–12	0.86
chloramphenicol	40/60	277	0.19	1–12	0.86
phenol	20/80	271	0.72	2–30	1.39
2,4-dichlorophenol	60/40	307	0.56	2–15	0.48
hydroquinone	5/95	291	0.36	1–12	0.57

Table S5 UPLC-MS/MS conditions for iodophenols

	Parent ion (m/z)	Transition monitored (m/z)	Retention time (min)	Collision energy (eV)	Formula	Structure
2-iodophenol	219	219 > 127	0.79	20	IC ₆ H ₄ OH	
3-iodophenol	219	219 > 127	0.88	20	IC ₆ H ₄ OH	
2,4,6-triiodophenol	471	471 > 127	2.39	35	I ₃ C ₆ H ₂ OH	

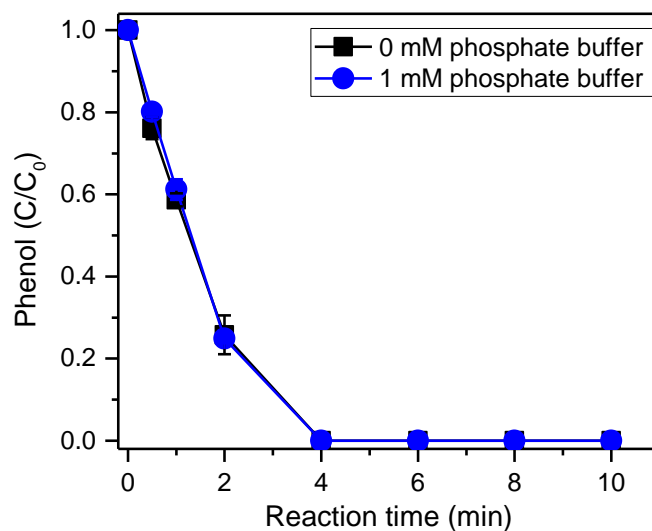


Figure S1. Effect of phosphate buffer on the degradation of phenol by PMS-I⁻ oxidation. Conditions: [phenol] = 10 μ M, [PMS] = 65 μ M, [NaH₂PO₄] = 1 mM, [Na₂SO₄] = 10 mM, and [I⁻] = 50 μ M.

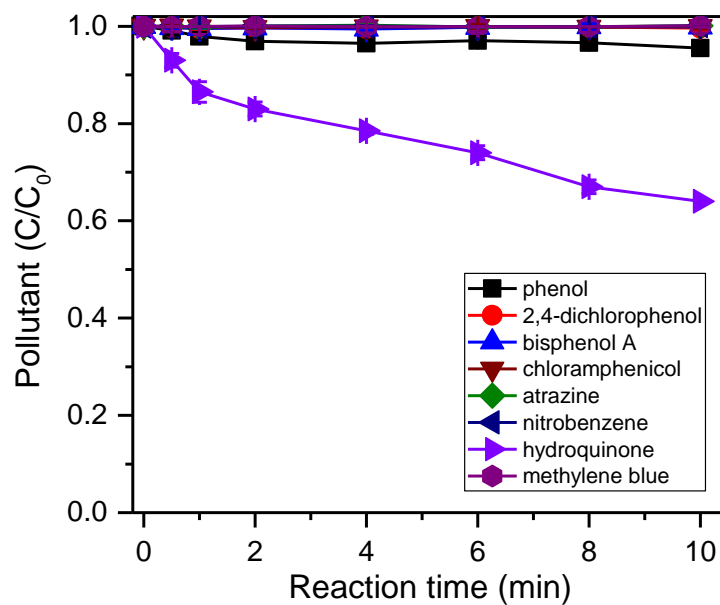


Figure S2. Degradation of pollutants by PMS alone. Conditions: [PMS] = 65 μ M, [phenol] = [2,4-dichlorophenol] = [bisphenol A] = [chloramphenicol] = [atrazine] = [nitrobenzene] = [methylene blue] = [hydroquinone] = 10 μ M, [Na₂SO₄] = 10 mM, and initial solution pH = 6.0.

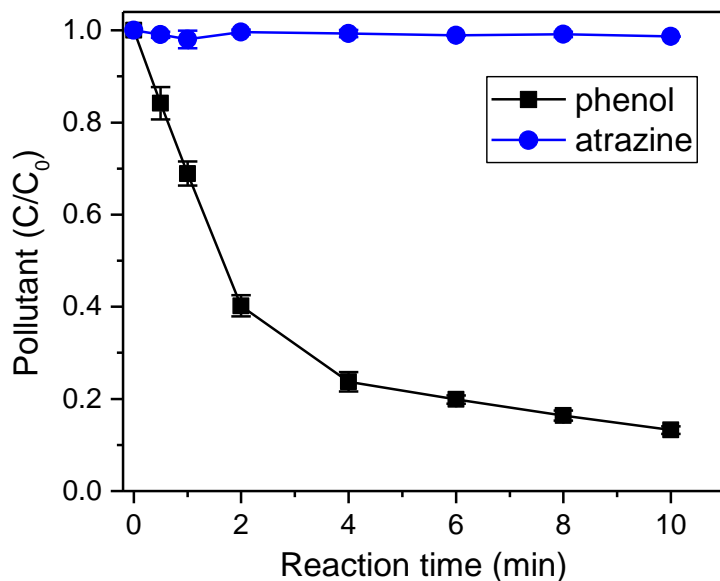


Figure S3. Concentrations of phenol and atrazine versus reaction time in PMS-I⁻ oxidation. Conditions: [PMS] = 65 μ M, [I⁻] = 50 μ M, [phenol] = [atrazine] = 25 μ M, [Na₂SO₄] = 10 mM, and initial solution pH = 6.0.

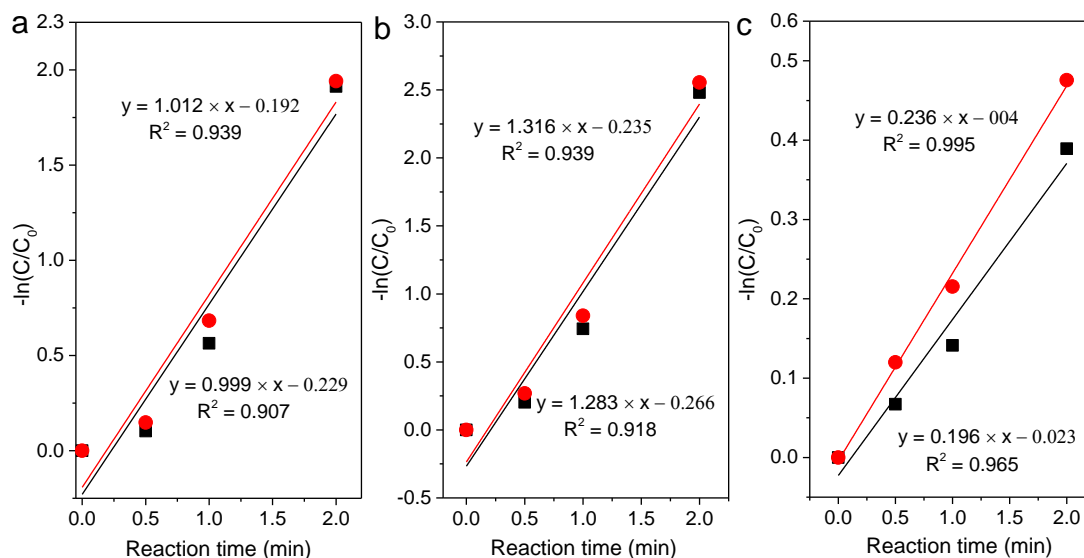


Figure S4. Plot of $-\ln(C/C_0)$ versus reaction time (min) during phenol (a), bisphenol A (b), and 2,4-dichlorophenol (c) degradation in PMS- I^- oxidation. Conditions: $[PMS] = 65 \mu M$, $[I^-] = 50 \mu M$, $[phenol] = [bisphenol A] = [2,4-dichlorophenol] = 10 \mu M$, $[Na_2SO_4] = 10 mM$, and initial solution pH = 6.0. Duplicate experiments were carried out and the slope represents the pseudo-first-order constant.

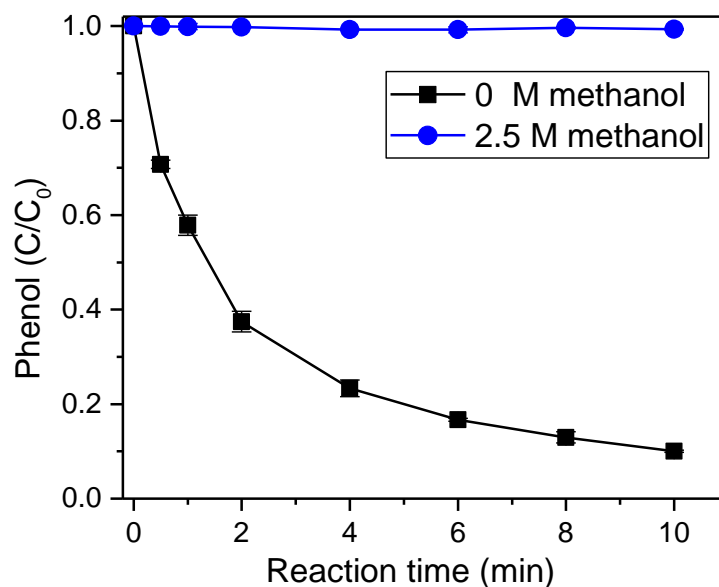


Figure S5. Effect of methanol on the degradation of phenol by PMS- Co^{2+} oxidation. Conditions: $[PMS] = 65 \mu M$, $[Co(NO_3)_2] = 65 \mu M$, $[phenol] = 25 \mu M$, and initial solution pH = 6.0.

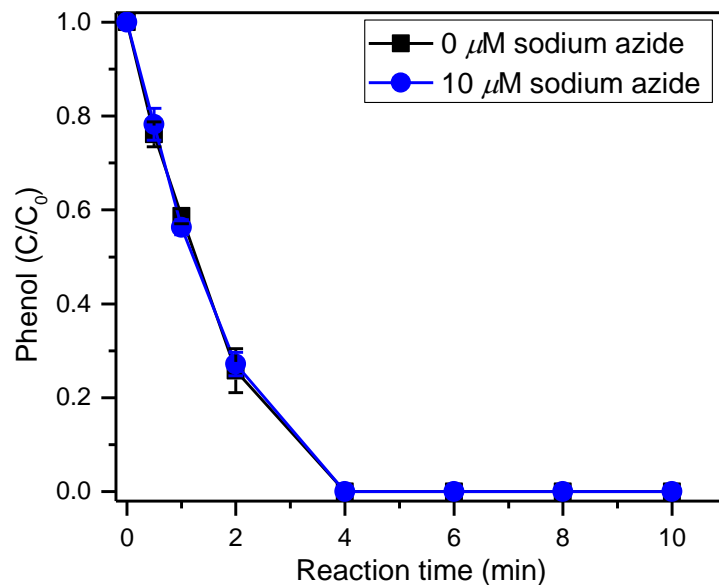


Figure S6. Effect of sodium azide on the degradation of phenol by PMS- I^- oxidation. Conditions: $[\text{PMS}] = 65 \mu\text{M}$, $[\text{I}^-] = 50 \mu\text{M}$, $[\text{phenol}] = 10 \mu\text{M}$, $[\text{sodium azide}] = 10 \mu\text{M}$, $[\text{Na}_2\text{SO}_4] = 10 \text{ mM}$, and initial solution pH = 6.0.

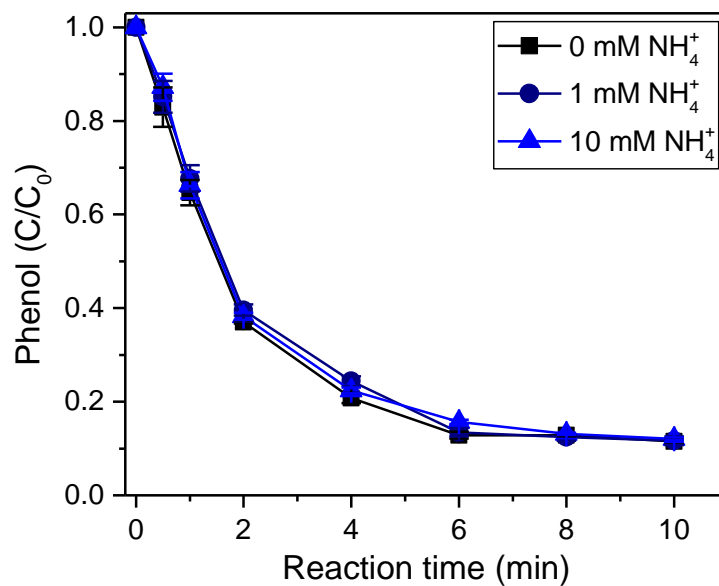


Figure S7. Effect of NH_4^+ on the degradation of phenol by PMS- I^- oxidation. Conditions: $[\text{PMS}] = 65 \mu\text{M}$, $[\text{I}^-] = 50 \mu\text{M}$, $[\text{phenol}] = 25 \mu\text{M}$, and $[\text{Na}_2\text{SO}_4] = 10 \text{ mM}$. The solution pH value was adjusted to 6.0 after adding $(\text{NH}_4)_2\text{SO}_4$.

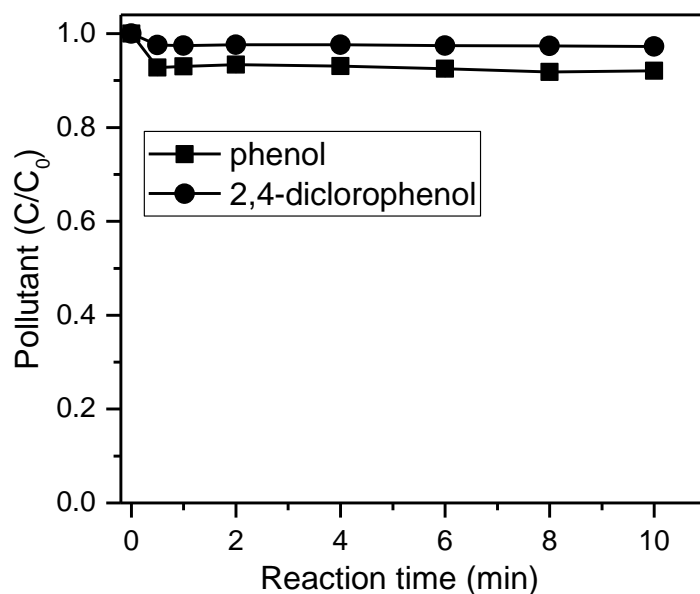


Figure S8. Degradation of phenols by PMS- I^- oxidation when a significant excess of I^- was present. Conditions: $[\text{PMS}] = 65 \mu\text{M}$, $[\text{I}^-] = 10 \text{ mM}$, $[\text{phenol}] = [\text{2,4-dichlorophenol}] = 10 \mu\text{M}$, $[\text{Na}_2\text{SO}_4] = 10 \text{ mM}$, and initial solution pH = 6.0.

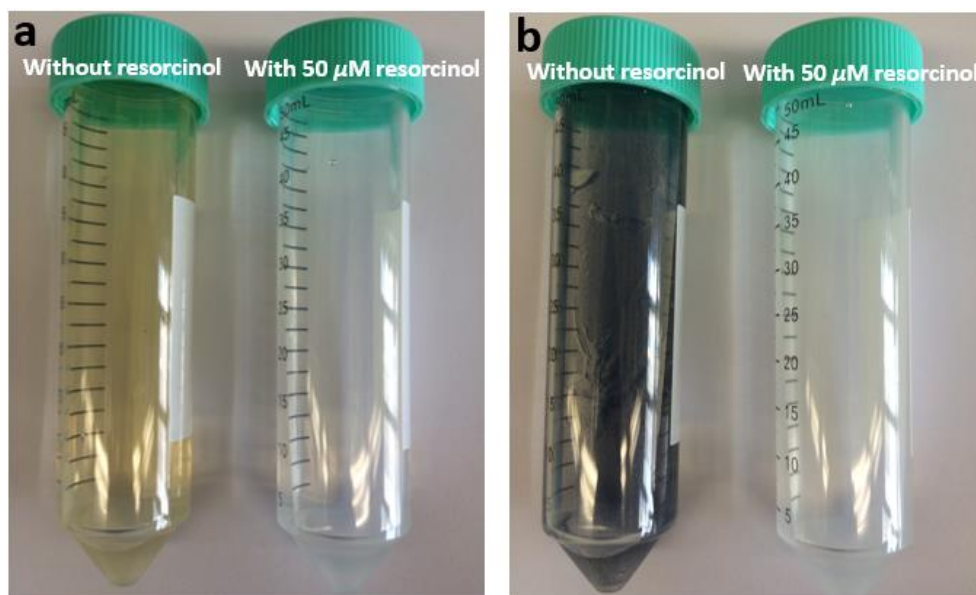


Figure S9. (a) Effect of resorcinol on the color of PMS- I^- oxidation and (b) the reactors in (a) after adding starch; the yellow color indicates the formation of I_3^- and the obvious color variation after adding starch indicates the presence of I_3^- . Conditions: $[\text{PMS}] = 100 \mu\text{M}$, $[\text{I}^-] = 500 \mu\text{M}$, $[\text{starch}] = 1 \text{ g L}^{-1}$, reaction time = 10 min, $[\text{Na}_2\text{SO}_4] = 10 \text{ mM}$, and initial solution pH = 6.0.

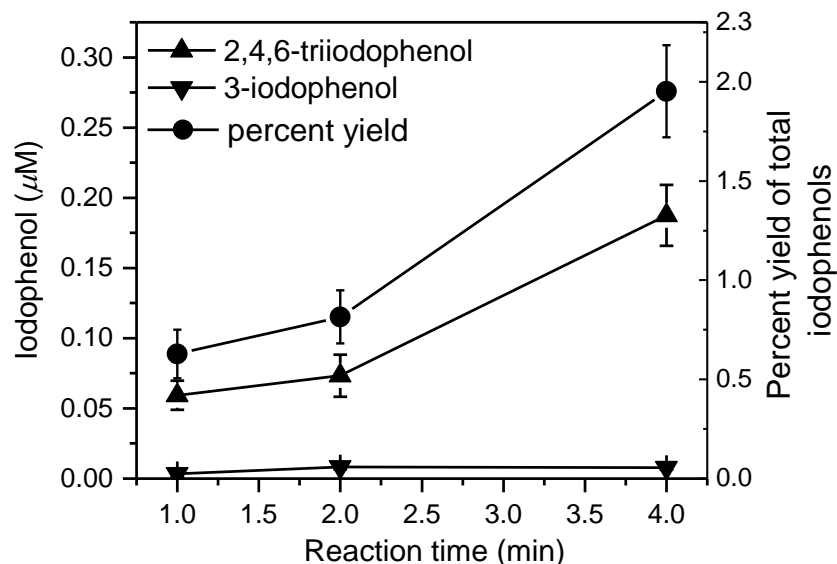


Figure S10. Profile of major iodinated intermediates produced during phenol degradation by PMS- I^- oxidation and their percent yield. Conditions: $[\text{PMS}] = 65 \mu\text{M}$, $[\text{I}^-] = 50 \mu\text{M}$, $[\text{phenol}] = 10 \mu\text{M}$, $[\text{Na}_2\text{SO}_4] = 10 \text{ mM}$, and initial solution pH = 6.0.

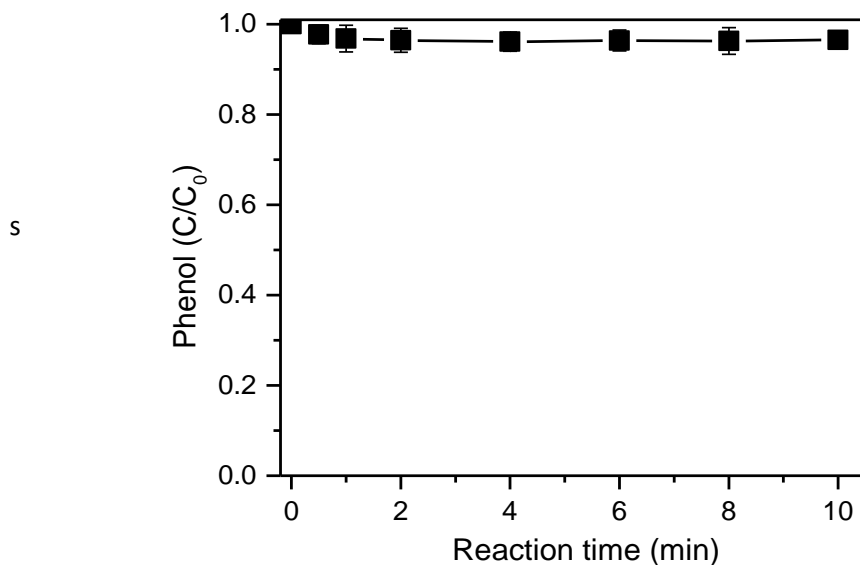


Figure S11. Phenol degradation in PMS solution in the presence of both Br^- and I^- . Conditions: $[\text{PMS}] = 65 \mu\text{M}$, $[\text{Br}^-] = 3.65 \mu\text{M}$, $[\text{I}^-] = 0.5 \mu\text{M}$, $[\text{phenol}] = 25 \mu\text{M}$, $[\text{Na}_2\text{SO}_4] = 10 \text{ mM}$, and initial solution pH 6.0; the doses of Br^- and I^- were based on their maximum weight ratios in the supplied sodium chloride (0.001% I^- and 0.01% Br^-) under the condition of 50 mM Cl^- .

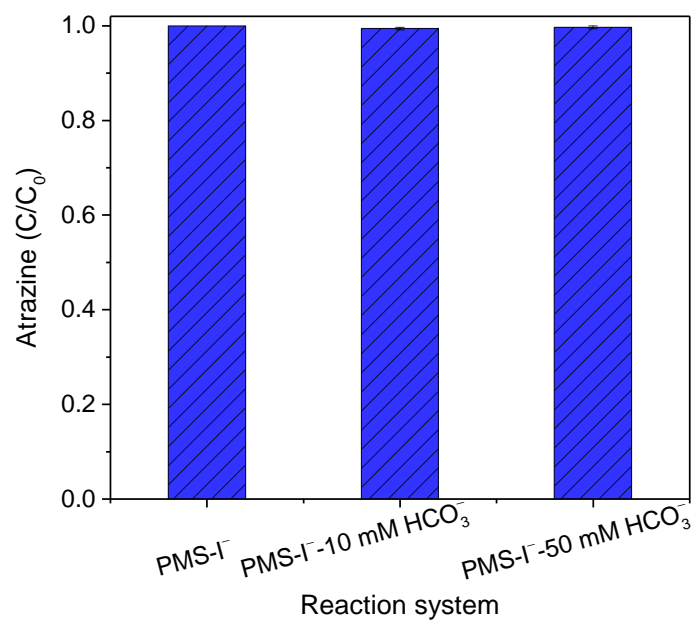


Figure S12. Effect of HCO_3^- on atrazine degradation in PMS- I^- oxidation. Conditions: $[\text{PMS}] = 65 \mu\text{M}$, $[\text{I}^-] = 50 \mu\text{M}$, $[\text{atrazine}] = 10 \mu\text{M}$, $[\text{Na}_2\text{SO}_4] = 10 \text{ mM}$, and reaction time = 10 min. The solution pH value was adjusted to 6.0 after adding HCO_3^- .

REFERENCES

- (1) Atkins, P., Physical Chemistry. 6th ed. Oxford University Press: Oxford, 1998; p 836.
- (2) Zhou, X.; Mopper, K., Determination of photochemically produced hydroxyl radicals in seawater and freshwater. *Mar. Chem.* **1990**, *30*, 71-88.
- (3) Moran, J. E.; Oktay, S. D.; Santschi, P. H., Sources of iodine and iodine 129 in rivers. *Water Resour. Res.* **2002**, *38* (8), 24-1–24-10.
- (4) Gibbs, R. J., Water chemistry of the Amazon River. *Geochim. Cosmochim. Acta* **1972**, *36* (9), 1061-1066.
- (5) Flury, M.; Papritz, A., Bromide in the natural environment: Occurrence and toxicity. *J. Environ. Qual.* **1993**, *22* (4), 747-758.
- (6) Zhang, E.; Wang, Y.; Qian, Y.; Ma, T.; Zhang, D.; Zhan, H.; Zhang, Z.; Fei, Y.; Wang, S., Iodine in groundwater of the North China Plain: Spatial patterns and hydrogeochemical processes of enrichment. *J. Geochem. Explor.* **2013**, *135*, 40-53.
- (7) Voutchkova, D. D.; Kristiansen, S. M.; Hansen, B.; Ernstsén, V.; Sørensen, B. L.; Esbensen, K. H., Iodine concentrations in Danish groundwater: Historical data assessment 1933-2011. *Environ. Geochem. Health* **2014**, *36* (6), 1151-64.
- (8) Thunqvist, E. L., Regional increase of mean chloride concentration in water due to the application of deicing salt. *Sci. Total Environ.* **2004**, *325* (1–3), 29-37.
- (9) Brindha, K.; Elango, L., Study on bromide in groundwater in parts of Nalgonda district, Andhra Pradesh. *Earth Sci. India* **2010**, *3* (1), 73-80.
- (10) Bagastyo, A. Y.; Batstone, D. J.; Kristiana, I.; Gernjak, W.; Joll, C.; Radjenovic, J., Electrochemical oxidation of reverse osmosis concentrate on boron-doped diamond anodes at circumneutral and acidic pH. *Water Res.* **2012**, *46* (18), 6104-6112.
- (11) Al-Muzaini, S. M., A comparative study of the characterization of landfill leachate at the dumping sites in Kuwait. *J. Food Agric. Environ.* **2009**, *7* (3&4), 679-683.
- (12) Di Palma, L.; Ferrantelli, P.; Merli, C.; Petrucci, E., Treatment of industrial landfill leachate by means of evaporation and reverse osmosis. *Waste Manage. (Oxford)* **2002**, *22* (8), 951-955.
- (13) Stumm, W.; Morgan, J. J., Aquatic chemistry: Chemical equilibria and rates in natural waters. 3th ed. John Wiley & Sons, 1995.

- (14) Harkness, J. S.; Dwyer, G. S.; Warner, N. R.; Parker, K. M.; Mitch, W. A.; Vengosh, A., Iodide, bromide, and ammonium in hydraulic fracturing and oil and gas wastewaters: Environmental implications. *Environ. Sci. Technol.* **2015**, *49* (3), 1955-1963.
- (15) Warner, N. R.; Kresse, T. M.; Hays, P. D.; Down, A.; Karr, J. D.; Jackson, R. B.; Vengosh, A., Geochemical and isotopic variations in shallow groundwater in areas of the Fayetteville Shale development, north-central Arkansas. *Appl. Geochem.* **2013**, *35*, 207-220.
- (16) Sambe, H.; Hoshina, K.; Hosoya, K.; Haginaka, J., Simultaneous determination of bisphenol A and its halogenated derivatives in river water by combination of isotope imprinting and liquid chromatography–mass spectrometry. *J. Chromatogr. A* **2006**, *1134* (1), 16-23.
- (17) Hoigné, J.; Bader, H., Rate constants of reactions of ozone with organic and inorganic compounds in water—II. *Water Res.* **1983**, *17* (2), 185-194.
- (18) Perrin, D. D., Ionisation constants of inorganic acids and bases in aqueous solution. 2th ed. Pergamon Press, 1982.
- (19) Zhao, Z.; Sun, W.; Yang, X.; Ye, X.; Wu, Y., Study of the catalytic behaviors of concentrated heteropolyacid solution. I. A novel catalyst for isobutane alkylation with butenes. *Catal. Lett.* **2000**, *65* (1-3), 115-121.
- (20) Oliveira, R.; Koskinen, W.; Ferreira, F., Sorption and leaching potential of herbicides on Brazilian soils. *Weed Res.* **2001**, *41* (2), 97-110.
- (21) Shi, X.; Wu, A.; Zheng, S.; Li, R.; Zhang, D., Molecularly imprinted polymer microspheres for solid-phase extraction of chloramphenicol residues in foods. *J. Chromatogr. B* **2007**, *850* (1), 24-30.
- (22) Herrero- Martínez, J. M.; Sanmartin, M.; Rosés, M.; Bosch, E.; Ràfols, C., Determination of dissociation constants of flavonoids by capillary electrophoresis. *Electrophoresis* **2005**, *26* (10), 1886-1895.
- (23) Neta, P.; Huie, R. E.; Ross, A. B., Rate constants for reactions of inorganic radicals in aqueous solution. *J. Phys. Chem. Ref. Data* **1988**, *17* (3), 1027-1284.
- (24) Neta, P.; Huie, R. E., Free-radical chemistry of sulfite. *Environ. Health Perspect.* **1985**, *64* 209.
- (25) Das, T. N., Reactivity and role of SO_5^- radical in aqueous medium chain oxidation of sulfite to sulfate and atmospheric sulfuric acid generation. *J. Phys. Chem. A* **2001**, *105* (40), 9142-9155.

(26) Deister, U.; Warneck, P., Photooxidation of sulfite (SO_3^{2-}) in aqueous solution. *J. Phys. Chem.* **1990**, *94* (5), 2191-2198.